Sympathetic neural inhibition of conducted vasodilatation along hamster feed arteries: complementary effects of α_1- and α_2-adrenoreceptor activation

Sara J. Haug[1,3] and Steven S. Segal[1,2,3]

[1] *The John B. Pierce Laboratory, 290 Congress Avenue, New Haven, CT 06519, USA*

[2] *Department of Cellular and Molecular Physiology, Yale University School of Medicine, New Haven, CT 06520, USA*

[3] *Department of Biomedical Engineering, Yale University, New Haven, CT 06520, USA*

Vasodilatation initiated on arterioles of skeletal muscle ascends into the proximal feed arteries through cell-to-cell conduction along the endothelium and into smooth muscle. Whereas perivascular sympathetic nerve activity (SNA) can inhibit conducted vasodilatation and restrict muscle blood flow, the signalling events mediating this interaction are poorly defined. Therefore, using isolated pressurized (75 mmHg) feed arteries (diameter (μm) at rest $= 53 \pm 3$; maximum $= 99 \pm 2$; $n = 86$) of the hamster retractor muscle, we tested the hypothesis that distinct yet complementary signalling pathways underlie the ability of SNA to inhibit conduction. Conducted vasodilatation was initiated using ACh microiontophoresis (1 μA; 250, 500 and 1000 ms) and SNA was initiated using local field stimulation (30–50 V; 1 ms at 2, 8 and 16 Hz). With vasodilatations of 5–20 μm, conduction increased with ACh pulse duration and was inhibited progressively as the frequency of SNA increased. During SNA, conduction was partially restored with inhibition of α_1- (0.1 μM prazosin) or α_2- (0.1 μM RX821002) adrenoreceptors and fully restored with both antagonists present. Activating α_1- (50 nM phenylephrine) or α_2- (1 μM UK 14,304) adrenoreceptors inhibited conduction partially and their simultaneous activation inhibited conduction cumulatively ($P < 0.05$). Elevated $[K^+]_o$ (30 or 40 mM) or phorbol esters (0.5 μM) also inhibited conduction yet similar constriction with L-NNA (50 μM) or Bay K 8644 (10 nM) did not. Thus, the activation of α_1- and α_2-adrenoreceptors inhibits conducted vasodilatation through complementary signalling events. With robust coupling along the endothelium, our modelling predicts that the inhibition of conduction by SNA can be explained by reduced electrical coupling through myoendothelial gap junctions or greater current leak across smooth muscle cell membranes.

The control of skeletal muscle blood flow is distributed among feed arteries external to the muscle and the arteriolar network embedded within striated muscle fibres. In response to muscle contractions, vasodilatation 'ascends' from arterioles into their arterial supply (Hilton, 1959; Folkow *et al.* 1971). With feed arteries positioned to govern the total amount of blood flowing into the muscle, dilatation of these proximal sites of resistance is required to achieve the full expression of functional hyperaemia (Williams & Segal, 1993; Segal & Jacobs, 2001). Ascending vasodilatation can be explained by cell-to-cell conduction of a dilator signal along the vessel wall (Hilton, 1959; Emerson & Segal, 2000b; Segal & Jacobs, 2001). For example, in feed arteries of the hamster retractor muscle, hyperpolarization is conducted along the endothelium and

into the surrounding smooth muscle through gap junction channels (Emerson & Segal, 2000a,b; Sandow *et al.* 2003).

Physical activity stimulates sympathetic nerve activation (SNA) to release noradrenaline, a powerful vasoconstrictor, at the same time that peripheral vasodilatation promotes blood flow into contracting muscles (Rowell *et al.* 1996; Thomas & Segal, 2004). In contrast to the robust conduction of vasodilatation from cell to cell along feed arteries, the coordination of vaso-constriction during SNA requires neurotransmitter release along perivascular sympathetic nerve fibres to activate adrenoreceptors on consecutive smooth muscle cells (Marshall, 1982; Welsh & Segal, 1996; Segal *et al.* 1999). In resting skeletal muscle, vasoconstriction increases with the level of SNA (VanTeeffelen & Segal, 2003).

However, vasodilator stimuli arising from contracting skeletal muscle can override smooth muscle contraction (Remensnyder *et al.* 1962), particularly in arterioles embedded within the active fibres, while vasoconstriction is sustained in feed arteries upstream (Folkow *et al.* 1971; Anderson & Faber, 1991; VanTeeffelen & Segal, 2003). The mechanism by which ascending vasodilatation of feed arteries is impaired during SNA is undefined.

Studies performed *in vivo* have shown that the conduction of vasodilatation along arterioles as well as feed arteries is suppressed during SNA (Kurjiaka & Segal, 1995; Haug *et al.* 2003). In a reciprocal manner, the conduction of vasodilatation can attenuate sympathetic vasoconstriction (Kurjiaka & Segal, 1995). These observations collectively suggest a functional interaction between SNA and conducted vasodilatation during the control of tissue blood flow that has remained unexplored. Whereas non-selective inhibition of α-adrenoreceptors prevents the ability of SNA to suppress conduction (Kurjiaka & Segal, 1995; Haug *et al.* 2003), α_1- and α_2-adrenoreceptors act through distinct signalling pathways (Bylund, 1992) and the role of these respective pathways in affecting conduction is unknown. Nor has it been determined whether single or multiple signalling events mediate the inhibitory actions of SNA on conducted vasodilatation.

Our goals in the present study were to define the functional interaction between SNA and conducted vasodilatation, and to distinguish the signalling events which mediate this interaction. Using isolated pressurized feed arteries of the hamster retractor muscle, an *in vitro* protocol was developed to provide greater control over the experimental environment than afforded previously *in vivo*. We tested the hypothesis that SNA inhibits conducted vasodilatation through distinct yet complementary adrenergic signalling pathways.

Methods

Animal care

Procedures were approved by the Animal Care and Use Committee of The John B. Pierce Laboratory and performed in accordance with the *Guide for the Care and Use of Laboratory Animals* of the National Research Council (USA). Male Golden hamsters ($n = 70$, 90–120 g; Charles River Breeding Laboratories, Kingston, NY, USA) were anaesthetized with pentobarbital sodium (65 mg kg^{-1}; I.P.). Following removal of feed arteries, the hamster was killed with an overdose of pentobarbital (I.P.).

Feed artery preparation

Physiological saline solution (PSS, pH 7.4) was prepared before each experiment and contained (mM): 148 NaCl,

4.7 KCl, 2.0 CaCl$_2$, 1.17 MgSO$_4$, 0.026 EDTA, 2.0 3-(*N*-morpholino) propanesulphonic acid, 5.0 glucose and 2.0 pyruvate dissolved in purified deionized water (dH$_2$O). These reagents were obtained from Sigma-Aldrich Chemical Co. (St Louis, MO, USA) and J.T. Baker (Phillipsburg, NJ, USA). This PSS was used to superfuse vessels throughout each experiment. To immerse vessels during microdissection, cannulation and to perfuse the vessel lumen, a second solution was made by adding albumin (10856, USB Corporation; Cleveland, OH, USA) to this PSS (final concentration, 1%).

To obtain feed arteries, an incision (~ 2 cm) was made through the skin over the scapula to expose the underlying retractor muscle of the cheek pouch. Using a stereo microscope (MZ8, Leica; Wetzlar, Germany), superficial connective tissue was removed and the muscle was reflected to access its vascular supply. Connective tissue and nerves around a feed artery and its adjacent collecting vein were carefully dissected away, then the vessel pair was severed at proximal and distal ends, and placed in a chilled (4°C) dissecting dish containing PSS. The vein was pinned at each end onto a Sylgard block (Dow Corning; Midland, MI, USA) and the feed artery was cleaned further of connective tissue, dissected away from the vein and transferred into a water-jacketed vessel chamber (1 ml, 4°C) and secured to a platform that contained a micro-manipulator at each end (MT-XYZ, Newport; Irvine, CA, USA).

A pair of heat-polished cannulation pipettes (outer diameter, 30–60 μm; one open and the other sealed) were pulled (P-97, Sutter Instruments; Novato, CA, USA) from borosilicate glass capillary tubes (GC150T-10, Warner Instruments; Hamden, CT, USA) and positioned in the vessel chamber using the respective micromanipulators. The open pipette was filled with PSS and connected to a hydrostatic column that was mounted on a vertical pulley to control transmural pressure. Using fine forceps, one end of the feed artery was pulled onto the pipette and secured with 11-0 monofilament nylon suture (7715, Ethicon; Somerville, NJ, USA). Pressure was raised to 10 cmH$_2$O to expel residual blood and the other end of the vessel was then secured onto the sealed pipette with 11-0 suture. Vessels were mounted without regard to their orientation *in vivo* (Emerson & Segal, 2000*a,b*, 2001); upstream and downstream refer to the direction of superfusion with PSS.

The cannulated vessel preparation was secured to a fixed stage that was positioned above an inverted microscope (TS100, Nikon; Garden City, NY, USA) mounted on a vibration isolation table (Technical Manufacturing Corporation; Peabody, MA, USA). Temperature and transmural pressure were raised gradually over 30 min to 35°C and 75 mmHg, respectively, with the vessel lengthened during pressurization to eliminate axial buckling. Final segment lengths were 3–5 mm. Vessels were superfused continuously

(3–4 ml min^{-1}) along their axes with fresh PSS; effluent was removed continuously by vacuum to maintain a constant fluid volume within the chamber. The integrity of smooth muscle cells was ascertained by the development of spontaneous myogenic tone, which averaged 53% of maximal diameter as determined with 10 μm sodium nitroprusside added to the PSS (SNP, Sigma-Aldrich).

Microiontophoresis

Stimulus micropipettes were pulled from borosilicate glass (GC120F-10, Warner; tip diameter, 1–2 μm) and filled with filtered (0.2 μm) ACh (1.0 m in dH$_2$O). The tip of a micropipette was positioned adjacent to the vessel using a micromanipulator (MN-151; Narishige, Japan) and a single pulse (500 ms, 1 μA) was delivered to verify endothelial cell viability upon vasodilatation (Emerson & Segal, 2000*b*; Haug *et al.* 2003). Based upon preliminary experiments, three levels of ACh stimulation at 1 μA (250, 500 and 1000 ms pulse) were used to characterize the interaction of conducted vasodilatation with SNA. Based upon these results (Fig. 1), the ACh stimulus was maintained at 500 ms, 1 μA in subsequent experiments. Retaining current was typically 200 nA to prevent leakage of ACh from the stimulus micropipette. Control experiments verified that vasodilatation no longer occurred when the ACh stimulus micropipette was positioned > 50 μm from the vessel wall, confirming the localized nature of this stimulus (Emerson & Segal, 2000*a,b*; Looft-Wilson *et al.* 2004).

Sympathetic nerve activation

A localized electric field was generated between two platinum wires (diameter, 250 μm) inserted into a Sylgard block at one end of the vessel chamber. The wires were positioned on either side of the feed artery at its downstream end, which was beyond the length of vessel used to evaluate local and conducted responses to ACh (illustrated in Fig. 1). Each wire was connected to respective poles of a stimulation isolation unit (SIU5, Grass; Quincy, MA, USA) driven by a monopolar square wave stimulator (S48, Grass). Based upon preliminary experiments, stimulus pulses (1 ms) were delivered at 'low' (2 Hz), 'medium' (8 Hz) and 'high' (16 Hz) frequencies at 30–50 V for 1–3 min to produce stable constrictions along the entire vessel (longer stimulation periods were necessary to maintain steady-state diameter during SNA at lower frequencies). A separate period of SNA was used for each ACh stimulus (see Experimental design). We confirmed that only vasoconstriction occurs during the activation of these perivascular nerves, with smooth muscle contraction mediated through noradrenergic neurotransmission (Welsh & Segal,

1996; Emerson & Segal, 2001; VanTeeffelen & Segal, 2003). Further, in denervated feed arteries ($n = 3$), we found no response to nerve stimulation while resting tone and constriction to phenylephrine (0.1 nm –1 μm) were preserved (Looft-Wilson *et al.* 2004).

Video microscopy

The inverted microscope rested on an *X–Y* translation stage which enabled repositioning of the field of view along the vessel without disturbing the preparation or micropipettes. Images were acquired using a Nikon 20× objective (numerical aperture = 0.50) with brightfield illumination provided by a 100 W halogen lamp. The image was projected onto a video camera (KP-D50, Hitachi; Japan) and displayed on a video monitor (PVM-1343 MD, Sony; Japan) at a total magnification of ×900. Internal diameter was measured (spatial resolution, ∼1 μm) using a video calliper (Microcirculation Research Institute; College Station, TX, USA). The output of the calliper was directed to a data acquisition system (Digidata 1322A, Axon Instruments, Union City, CA, USA) using pCLAMP software (Version 8.1; Axon) and sampled at 333 Hz.

Vasomotor responses

Vasomotor responses to ACh and SNA are presented as 'Diameter change' (ΔD), which was calculated as the peak response diameter minus the preceding resting baseline diameter. Responses were evaluated locally at the site of stimulation and at defined distances (determined with a calibrated eyepiece reticule) along 2 mm of the vessel upstream from the ACh stimulus. To initially characterize the interaction between SNA and conducted vasodilatation, sites were observed at 1000 and 2000 μm upstream (see Fig. 1). In subsequent experiments, two additional sites (500 and 1500 μm upstream) were also observed to enhance the resolution of effects produced by experimental interventions. The order in which respective sites were studied along a vessel was randomised across experiments. At the end of each day, maximum vessel diameter was determined with SNP.

Pharmacological reagents

Pharmacological reagents were prepared for use on the day of an experiment. Each reagent was diluted to the desired concentration in the superfusion solution. All compounds were obtained from Sigma-Aldrich, with the exception of prazosin, which was obtained from Research Biochemicals International (Natick, MA, USA).

Agonists. Preliminary studies were performed to determine concentrations of vasoactive agents which mimicked the magnitude of feed artery constriction

to 8 Hz SNA. Thus, efficacy was defined from a functional perspective in order to achieve similar levels of vasoconstriction (Tables 1 and 2) and differences in the ability of respective stimuli to inhibit conducted vasodilatation were interpreted as reflecting differences in their mode of action. These agents include [−]-noradrenaline (non-specific adreno-receptor agonist, 0.1 μM), phenylephrine (selective α_1-adrenoreceptor agonist, 50 nM), angiotensin II (AT1 receptor agonist, 50 pM), phorbol 12,13-dibutyrate (PDB,

protein kinase C activator, 0.5 μM), phorbol 12-myristate 13-acetate (PMA, protein kinase C activator, 0.5 μM) and Bay K 8644 (L-type Ca^{2+} channel opener; 10 nM). The selective α_2-adrenoreceptor agonist, UK 14,304 (Aburto *et al.* 1993) was used at 1 μM; preliminary experiments indicated that UK 14,304 had no further effects at 10 or 100 μM.

Antagonists. Concentrations of phentolamine (non-selective α-adrenoreceptor antagonist, 1 μM),
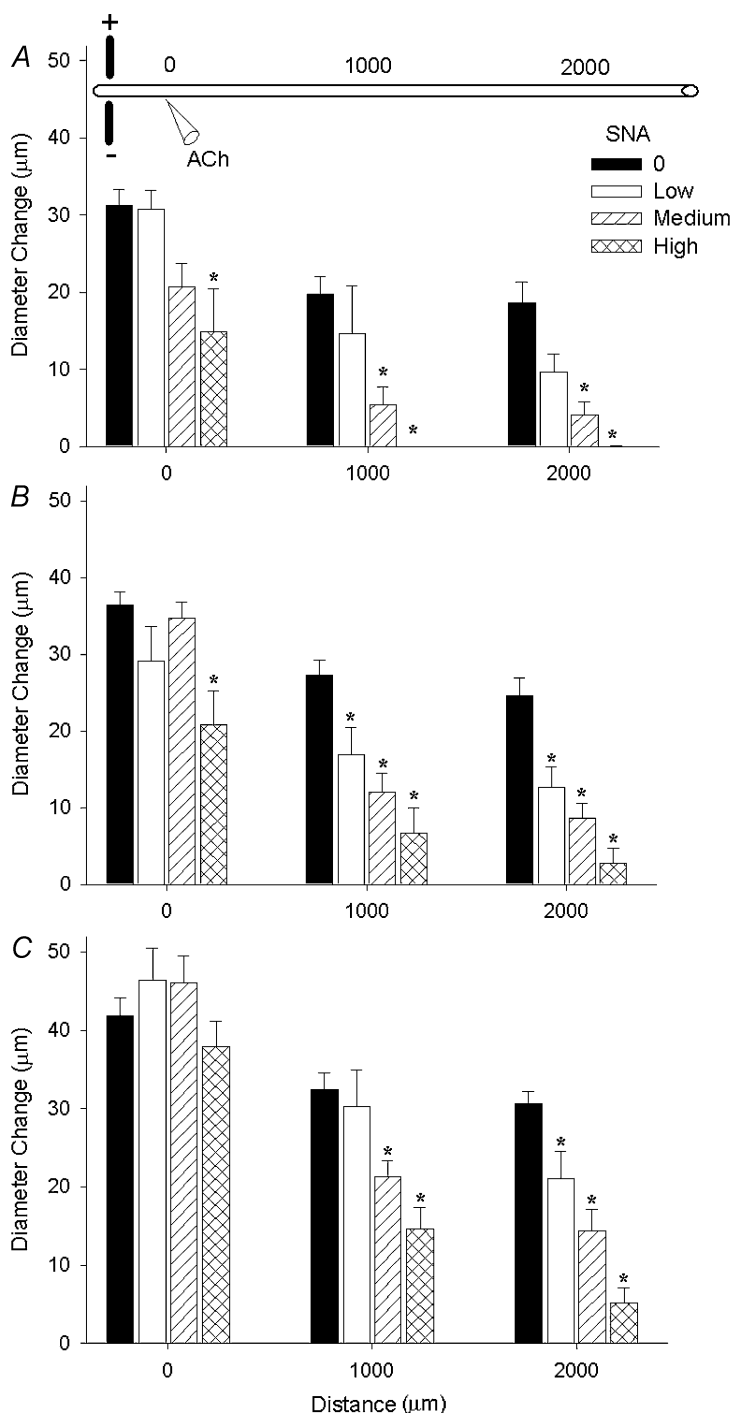

Figure 1. Conducted vasodilatation to ACh is attenuated during SNA
Conducted vasodilatation was triggered by *A*, 250 ms; *B*, 500 ms, or *C*, 1000 ms pulses of ACh (each at 1 μA) and evaluated during control conditions ('0') and during 'Low' (2 Hz), 'Medium' (8 Hz) and 'High' (16 Hz) levels of SNA with $n = 6$–9 vessels in each condition. As depicted in the illustration at the top of the figure (and applies to Figs 1–5), distance refers to that along the feed artery from site of ACh stimulation at '0' μm. Flow of PSS during superfusion was from right to left with Pt electrodes for SNA ('+' and '−') positioned across downstream end. A General Linear Model analysis indicated that the overall model was highly significant (d.f. = 13, $F = 53.83$, $P < 0.0001$). There were significant main effects of distance (d.f. = 2, $F = 143.58$, $P < 0.0001$), SNA level (d.f. = 3, $F = 72.65$, $P < 0.0001$) and ACh stimulus level (d.f. = 2, $F = 79.85$, $P < 0.0001$). However, there was no significant interaction between levels of ACh and SNA (d.f. = 6, $F = 1.38$, $P = 0.22$). *Significant difference from respective control responses to ACh with '0' SNA ($P < 0.05$) using Tukey's *post hoc* comparisons. Note that raising the level of SNA abolished conduction in response to 250 ms ACh (panel *A*), while conduction persisted during SNA when the ACh stimulus was raised to 500 and 1000 ms (panels *B* and *C*).

Table 1. Feed artery diameter at rest, during sympathetic nerve activity (SNA) and during SNA with pharmacological treatment

Treatment	1000 μm						2000 μm					
	Rest (μm)	Rest (%)	SNA (μm)	SNA (%)	SNA + treatment (μm)	SNA + treatment (%)	Rest (μm)	Rest (%)	SNA (μm)	SNA (%)	SNA + treatment (μm)	SNA + treatment (%)
Phentolamine (1 μM)	57 ± 10	55 ± 4	44 ± 6*	43 ± 3*	55 ± 10	54 ± 5	55 ± 7	54 ± 3	42 ± 5*	43 ± 4*	56 ± 5	55 ± 3
Propranolol (1 μM) †	57 ± 5	55 ± 3	47 ± 6*	45 ± 4*	49 ± 5*	47 ± 4*	54 ± 5	52 ± 3	43 ± 5*	41 ± 3*	45 ± 6*	43 ± 4*
Prazosin (0.1 μM)	53 ± 5	55 ± 4	42 ± 5*	44 ± 6*	51 ± 4	53 ± 5	55 ± 5	57 ± 4	44 ± 5*	46 ± 5*	54 ± 4	56 ± 4
RX821002 (0.1 μM)	66 ± 7	59 ± 3	54 ± 6*	48 ± 2*	57 ± 7	51 ± 3	62 ± 8	55 ± 4	50 ± 4*	45 ± 3*	56 ± 8	50 ± 4

Diameter measures are given as absolute (μm) and as per cent of maximal diameter (%) at rest, during 8 Hz SNA (∼1–3 min) and during either 8 Hz SNA (∼1 min) or the stimulus indicated. Summary data are means ± S.E.M. (n = 5–9 vessels per cell). Values were recorded at the midpoint (1000 μm) and at the furthest distance of observation (2000 μm) along vessel segments. From 2-way ANOVA, F ratios ($P < 0.05$) were 6.2–17.6 with 2 d.f. *Post hoc* comparisons: *significant difference from rest ($P < 0.05$). † Main effect of distance ($P < 0.05$) attributable to slight and consistent difference between 1000 and 2000 μm.

Table 2. Feed artery diameter at rest and during stimulation

Stimulus	1000 μm				2000 μm			
	Rest (μm)	Rest (%)	Stimulus (μm)	Stimulus (%)	Rest (μm)	Rest (%)	Stimulus (μm)	Stimulus (%)
SNA (8 Hz)	52 ± 4	55 ± 3	41 ± 3*	44 ± 2*	48 ± 4	51 ± 3	39 ± 4*	41 ± 3*
Noradrenaline (0.1 μM)	48 ± 7	53 ± 3	36 ± 4*	41 ± 2*	47 ± 6	52 ± 3	36 ± 3*	41 ± 2*
Phenylephrine (50 nM)	63 ± 4	57 ± 3	52 ± 3*	47 ± 2*	62 ± 3	56 ± 3	53 ± 3*	48 ± 3*
UK 14,304 (1 μM)	49 ± 5	49 ± 3	51 ± 4	52 ± 2	50 ± 5	50 ± 4	46 ± 4	46 ± 3
Phenylephrine + UK 14,304	45 ± 6	51 ± 2	38 ± 6*	43 ± 3*	44 ± 6	50 ± 3	37 ± 4*	42 ± 2*
Angiotensin II (50 pM)	57 ± 8	56 ± 3	48 ± 8*	47 ± 3*	57 ± 8	56 ± 3	46 ± 8*	45 ± 4*
PMA (0.5 μM)	68 ± 3	57 ± 4	53 ± 4*	45 ± 4*	63 ± 2	53 ± 3	54 ± 1*	45 ± 2*
PDB (0.5 μM)	47 ± 6	50 ± 3	40 ± 4*	43 ± 3*	49 ± 7	52 ± 5	41 ± 5*	44 ± 4*
30 mM KCl	56 ± 7	56 ± 4	44 ± 6*	44 ± 3*	54 ± 6	54 ± 3	38 ± 2*	38 ± 3*
40 mM KCl	53 ± 5	54 ± 3	35 ± 5*	36 ± 3*	52 ± 4	53 ± 3	31 ± 1*	31 ± 2*
Bay K 8644 (10 nM)	62 ± 6	56 ± 3	50 ± 7*	45 ± 5*	63 ± 5	57 ± 3	45 ± 2*	41 ± 2*
L-NNA (100 μM)	50 ± 3	49 ± 3	39 ± 2*	39 ± 4*	48 ± 3	47 ± 3	38 ± 2*	37 ± 3*

Diameter measures are given as absolute (μm) and as per cent of maximal diameter (%) at rest and during either SNA (8 Hz, 30–50 V, ∼1 min) or the stimulus indicated. Summary data are means ± S.E.M. (n = 5–9 vessels per cell). Values were recorded at the midpoint (1000 μm) and at the furthest distance of observation (2000 μm) along vessel segments. From 2-way ANOVA, F ratios ($P < 0.05$) were 9.707–59.8 with 1 d.f. *Post hoc* comparisons: *significant difference from rest ($P < 0.05$).

D,L-propranolol (β-adrenoreceptor antagonist, 1 μM), RX821002 (α_2-adrenoreceptor antagonist, 0.1 μM; Zhang *et al.* 2002), prazosin HCl (α_1-adrenoreceptor antagonist, 0.1 μM), calphostin C (protein kinase C antagonist, 0.1 μM), chelerythrine chloride (protein kinase C antagonist, 0.1 μM), N^{ω}-nitro-L-arginine (L-NNA, nitric oxide synthase inhibitor; 50 or 100 μM) and indomethacin (cyclooxygenase inhibitor; 100 μM) were determined based upon previous experience and published results.

Across experiments, up to three pharmacological interventions were performed per vessel. When two or three interventions were performed, they were done in a cumulative manner (e.g. inhibition of either α_1- or α_2-adrenoreceptor subtypes followed by inhibition of both subtypes in the presence of propranolol) and their order of administration was varied between experiments.

Experimental design

Interaction between conducted vasodilatation and SNA. To evaluate local and conducted vasodilatation, a separate ACh stimulus was delivered for each observation site. Responses to SNA were then evaluated at each site. Local and conducted responses to ACh were then re-evaluated during steady-state SNA, with a separate period of SNA

initiated prior to each ACh stimulus and maintained (~1–3 min) until the response to ACh recovered by at least 50%. Between each observation, vessels recovered for ~3 min to restore resting diameter and reactivity. After evaluating the effects of SNA on conduction, local and conducted vasodilatation were re-evaluated a final time and recovered consistently to initial control values ($n = 21$; data not shown). Preliminary studies established that tachyphylaxis to these stimulus protocols was negligible for the duration of an experiment (2–6 h).

Pharmacological interventions. After evaluating control responses to ACh (above), a pharmacological agent was then added to the superfusion solution and allowed to equilibrate for at least 10 min. Conducted responses to ACh were then re-evaluated in the presence of the agent. In some cases (described in context), local and conducted responses to ACh during SNA were also evaluated before and during treatment with pharmacological agents. All

diameter changes were evaluated from the prevailing base-line diameter. For example, during SNA or protein kinase C activation with phorbol ester, the vessel constricted and the baseline diameter was less than during control measurements. Controls for changes in baseline diameter are also described in context.

Mathematical modelling using NEURON

The NEURON simulation environment (Hines & Carnevale, 1997) was adapted to model passive current flow in microvascular networks (Crane *et al.* 2001). Control parameters within the model describing the resistive properties of membranes and of cell-to-cell coupling within and between endothelial and smooth muscle cell layers, were modified to reflect electro-physiological data obtained from feed arteries of the hamster retractor muscle (Emerson & Segal, 2000*a*) in accordance with the present data for conducted vasodilatation.
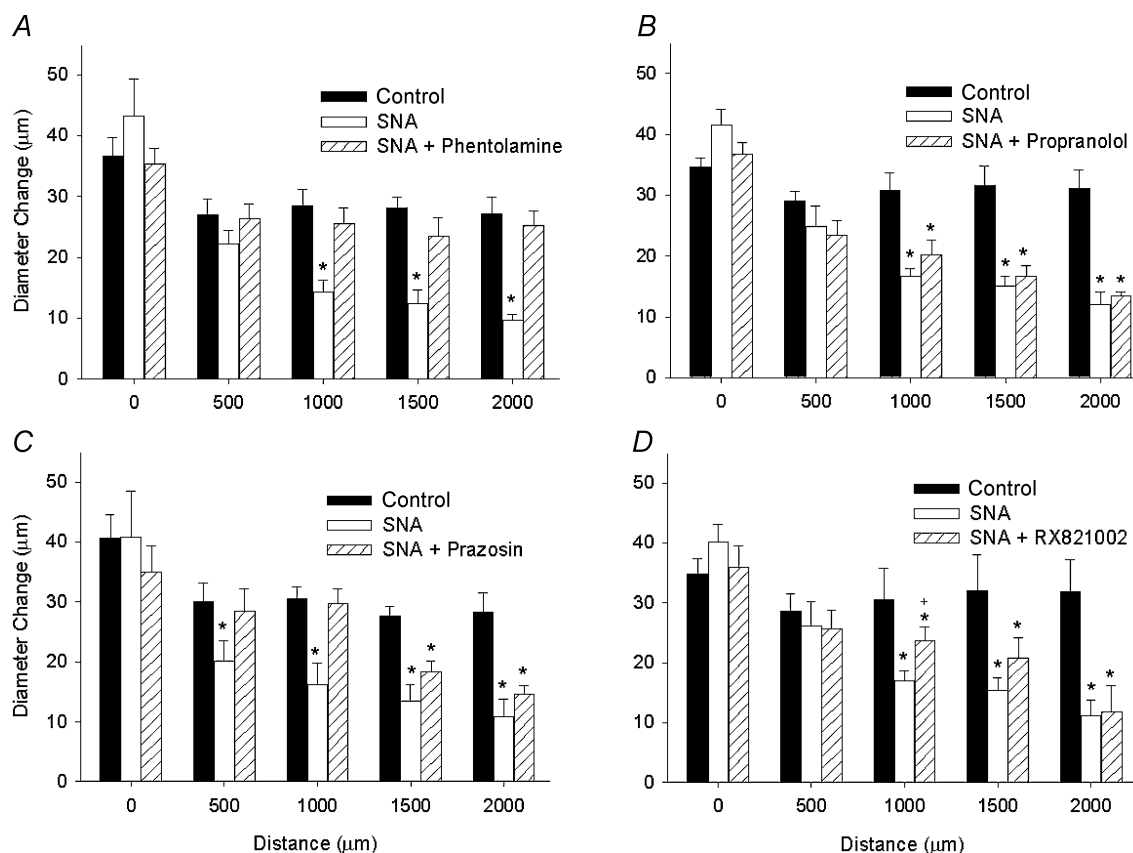

Figure 2. Inhibition of conducted vasodilatation during SNA is reversed through blockade of both α_1- and α_2-adrenoreceptors

In each of these experiments, across 3 conditions (control, SNA, SNA + treatment), there was significant main effect of distance on conducted vasodilatation (2-way ANOVA). *A*, phentolamine restored conducted vasodilatation to ACh during 8 Hz SNA ($n = 5$; d.f. = 8, $F = 7.366$, $P < 0.001$). *B*, propranolol had no effect on conducted vasodilatation during SNA ($n = 5$; d.f. = 8, $F = 9.398$, $P < 0.001$). *C*, conduction during SNA was partially restored by prazosin ($n = 5$; d.f. = 8, $F = 4.017$, $P = 0.004$). *D*, conduction during SNA was partially restored by RX821002 ($n = 5$; d.f. = 8, $F = 9.301$, $P < 0.001$). *Post hoc* comparisons: *significant difference from control response at sites indicated ($P < 0.05$); +significant difference from response during SNA at site indicated ($P < 0.05$).

Following simulated current injection into the endothelium, the passive spread and decay of hyperpolarization was modelled in both cell layers. Myoendothelial coupling resistance and smooth muscle membrane resistance were then varied to test how respective effects of SNA influence conduction. Outputs from the NEURON simulations were transferred to SigmaPlot (v. 8.0; SPSS, Chicago, IL, USA) for final presentation.

Data analysis and statistics

Vasomotor responses are expressed as the absolute diameter change (ΔD, μm) with summary values presented as means $\pm$ s.e.m. Typically one vessel (occasionally 2) was studied per hamster; 'n' refers to the number of vessels studied. To explore possible interactions between levels of SNA and ACh stimuli using our *in vitro* model, the data in Fig. 1 were analysed using a General Linear Model procedure (Statistical Analysis Software, version 8; SAS Institute, Cary, NC, USA). Summary data in Figs 2–5 and in Tables 1 and 2 were

analysed using one- and two-way analyses of variance (ANOVA) with a repeated measures design (SigmaStat, v. 3.0, SPSS). When significant F ratios were obtained (see figure captions), Tukey tests were performed for *post hoc* comparisons. To facilitate comparisons, tabled values are presented as actually measured (in μm) and normalized to respective maximal diameters. Differences were accepted as statistically significant with $P < 0.05$.

Results

A total of 86 vessels were studied from 70 hamsters; resting diameter following equilibration was 53 ± 3 μm and maximal diameter was 99 ± 2 μm.

Interaction between SNA and conducted vasodilatation

To characterize the interaction between SNA and conducted vasodilatation, three levels of ACh stimulation
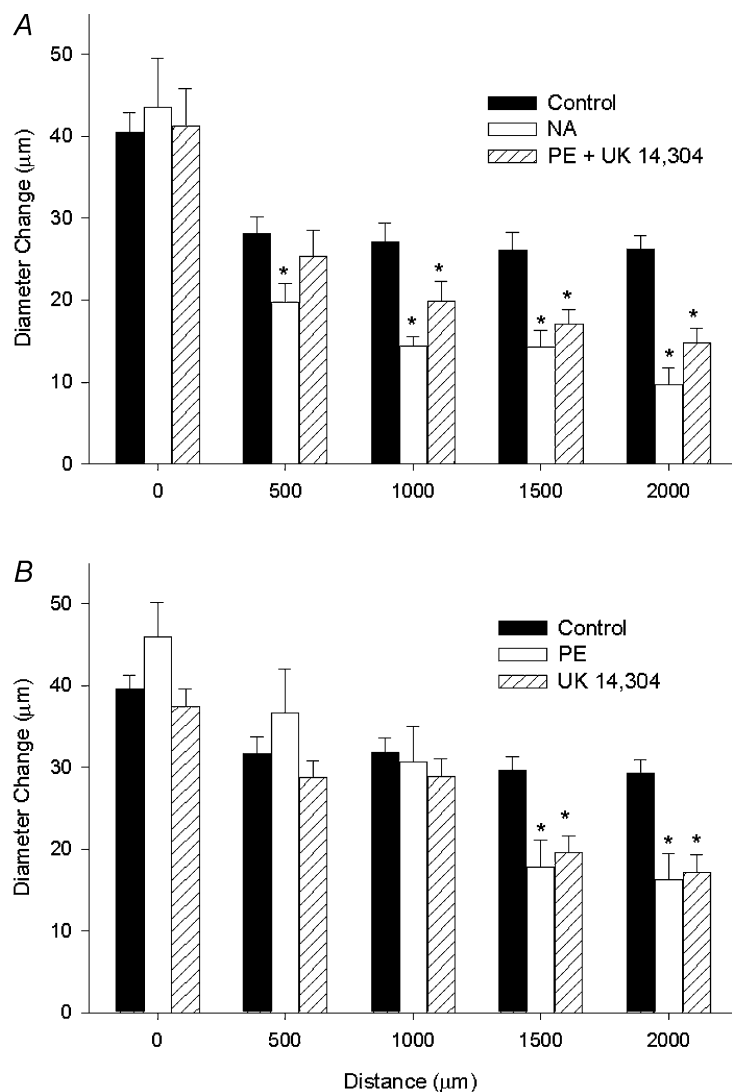

Figure 3. Simultaneous activation of α_1- and α_2-adrenoreceptors augments the inhibition of conducted vasodilatation
A, activation of α_1- and α_2-adrenoreceptors with noradrenaline (NA, $n = 5$) or phenylephrine (PE) + UK 14,304 together ($n = 5$) inhibits conducted vasodilatation similar to that observed during 8 Hz SNA (see Fig. 2). The effect of distance on conducted vasodilatation was significant with noradrenaline (d.f. = 4, $F = 15.098$, $P < 0.001$) and with PE + UK 14,304 (d.f. = 4, $F = 6.372$, $P = 0.005$). *B*, selective stimulation of α_1-adrenoreceptors with phenylephrine ($n = 7$) or of α_2-adrenoreceptors with UK 14,304 ($n = 8$) partially inhibits conducted vasodilatation. The effect of distance on conducted vasodilatation was significant with phenylephrine (d.f. = 4, $F = 13.352$, $P < 0.001$) and with UK 14,304 (d.f. = 4, $F = 3.292$, $P = 0.049$). *Post hoc* comparisons: *significant difference from control response at sites indicated ($P < 0.05$).

(250, 500 and 1000 ms pulse at 1 μA) were tested during three levels of perivascular nerve stimulation (2, 8 and 16 Hz) at a constant transmural pressure of 75 mmHg. Respective vasoconstrictions were 4 ± 1, 9 ± 1 and 17 ± 2 μm. The General Linear Model procedure indicates that the overall model is highly significant ($P < 0.0001$). Under control conditions, conducted vasodilatation was maintained with distance along the vessel (Fig. 1). The amplitudes of local and conducted vasodilatation increased significantly with the duration of the ACh stimulus. At each level of ACh stimulation, conducted vasodilatation decreased significantly as the level of SNA increased and this effect of SNA increased significantly with distance along the vessel. However, there was no significant interaction between the level of ACh stimulation and the level of SNA (see caption of Fig. 1 for details of statistical analysis). Throughout experiments, the effects of SNA on conducted vasodilatation were apparent even when there was no change in local vasodilatation (Fig. 1). Based upon this characterization, intermediate

levels of ACh microiontophoresis (500 ms, 1 μA) and SNA (8 Hz) were used for all subsequent experiments. The resting diameter of feed arteries and their baseline diameters during experimental interventions were similar along vessels; observations at 1000 and at 2000 μm are presented in Tables 1 and 2 for comparisons.

Distinct roles for α_1- and α_2-adrenoreceptors but not for β-adrenoreceptors

To resolve which general class of adrenoreceptor subtype (i.e. α versus β) mediates the attenuation of conducted vasodilatation by SNA, either propranolol or phentolamine was added to the superfusion solution. Sympathetic vasoconstriction was inhibited completely by phentolamine but not by propranolol (Table 1). Furthermore, phentolamine completely restored conducted vasodilatation during SNA (Fig. 2A) while propranolol had no effect on the inhibition of conduction during SNA (Fig. 2B).
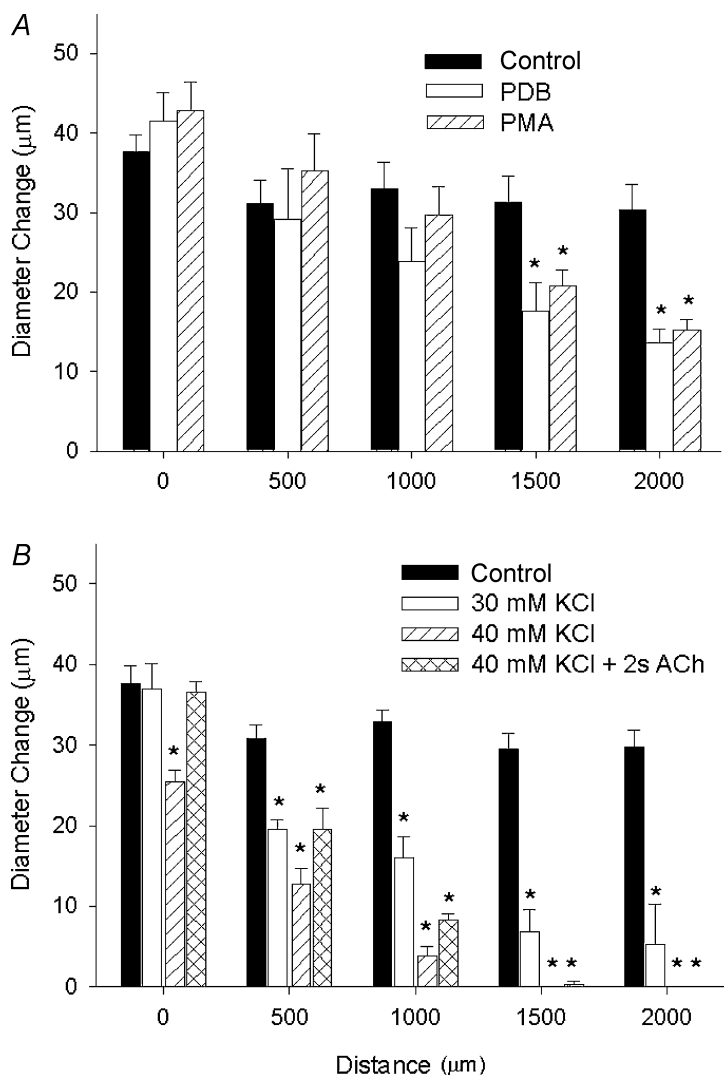

Figure 4. Stimulation with phorbol esters or depolarizing solutions of KCl attenuate conducted vasodilatation

A, in the presence of phorbol 12, 13-dibutyrate (PDB; $n = 5$) or phorbol 12-myristate 13-acetate (PMA; $n = 5$), conduction was attenuated at remote sites. The effect of distance on conducted vasodilatation was significant with PMA (d.f. = 4, $F = 10.863$, $P < 0.001$) and with PDB (d.f. = 4, $F = 14.176$, $P < 0.001$). B, raising $[K^+]_o$ to 30 or 40 mM abolished conducted vasodilatation ($n = 6$) even when local vasodilatation was maintained. The effect of distance on conducted vasodilatation was significant across KCl treatments (d.f. = 12, $F = 9.610$, $P < 0.001$). Post hoc comparisons: *significant difference from control response at sites indicated ($P < 0.05$).

Inhibition of α-adrenoreceptor subtypes. Vasoconstriction in response to SNA was inhibited completely during blockade of α_1-adrenoreceptors with prazosin and partially during blockade of α_2-adrenoreceptors with RX821002 (Table 1). Each of these interventions partially restored conducted vasodilatation during SNA (Fig. 2C and D, respectively). The combination of prazosin + RX821002 eliminated sympathetic vasoconstriction and completely restored conducted vasodilatation (observed at $2000\,\mu$m: control, $\Delta D = 28 \pm 3\,\mu$m; during $8\,$Hz SNA, $\Delta D = 11 \pm 3\,\mu$m, $P < 0.05$; during $8\,$Hz SNA + prazosin + RX821002, $\Delta D = 29 \pm 1\,\mu$m; $n = 5$).

Activation of α-adrenoreceptor subtypes. Exogenous noradrenaline or the combination of phenylephrine + UK 14,304 mimicked the ability of SNA to inhibit conducted vasodilatation (Fig. 3A). However, neither phenylephrine alone nor UK 14,304 alone attenuated conduction to the same extent as SNA or noradrenaline

(Fig. 3B; e.g. at the distance of $1000\,\mu$m, compare conducted responses under respective conditions with those for SNA in Fig. 2). Nevertheless, each agent significantly attenuated conducted vasodilatation (and did so to a similar extent) at the furthest distances along the vessel (Fig. 3B). Vasoconstrictions with noradrenaline or with phenylephrine mimicked the effect of SNA whereas UK 14,304 had no significant effect on resting diameter (Table 2).

Specificity controls. To control for possible non-selective activation of designated α-adrenoreceptor subtypes, four experiments with phenylephrine were performed in the presence of RX821002 and four experiments with UK 14,304 were performed in the presence of prazosin. As there was no difference in the partial attenuation of conduction in either condition, these data were pooled for respective agonists in Fig. 3B. To further test the specificity of UK 14,304 as an α_2-adrenoreceptor agonist, conduction to ACh was evaluated before and after
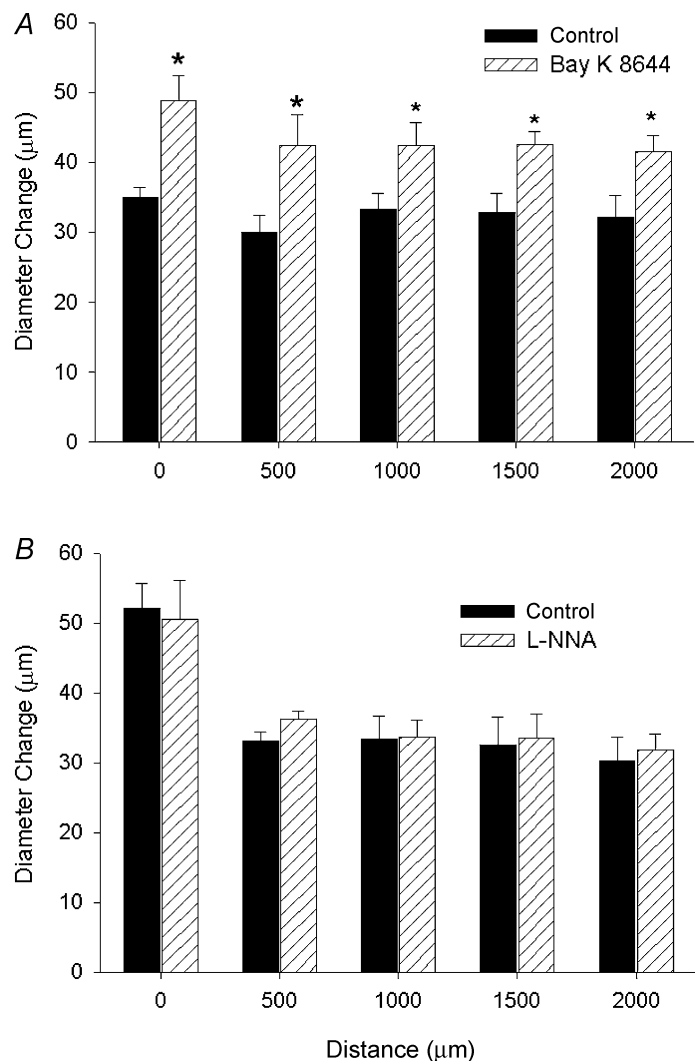

Figure 5. Vasoconstriction through activation of L-type Ca^{2+} channels or inhibition of nitric oxide synthase does not attenuate conducted vasodilatation
A, addition of Bay K 8644 constricted feed arteries (see Table 2) and augmented both local and conducted vasodilatation ($n = 5$). B, addition of L-NNA constricted feed arteries (see Table 2) with no effect on conducted vasodilatation ($n = 5$). Distance had no significant effect on conduction in the presence of Bay K 8644 (d.f. = 4, $F = 0.556$, $P = 0.697$) or L-NNA (d.f. = 4, $F = 0.479$, $P = 0.751$). *Post hoc* comparisons: *significant difference from control response at sites indicated ($P < 0.05$).

UK 14,304 was added to the superfusion solution (at 2000 μm: control, $\Delta D = 33 \pm 4 \, \mu$m; with UK 14,304, $\Delta D = 16 \pm 1 \, \mu$m; $P < 0.05$). RX821002 was then added with UK 14,304 and conducted vasodilatation was fully restored ($\Delta D = 34 \pm 5 \, \mu$m; $n = 4$).

Signalling events initiated through α-adrenoreceptor activation

Stimulation of the α_1-adrenoreceptor activates the G_q-protein-coupled signalling pathway, resulting in activation of protein kinase C (Exton, 1985; Taguchi *et al.* 1998). The binding of angiotensin II to the AT_1 receptor can also stimulate this pathway (Dinh *et al.* 2001) and was used as an independent stimulus for evaluating the effect of G_q activation on conducted vasodilatation. With a similar level of vasoconstriction (Table 2), angiotensin II attenuated conduction in the manner observed with phenylephrine (refer to Fig. 3*B*): there was no significant effect along the first 1000 μm but conducted responses were attenuated at greater distances (e.g. at 2000 μm: control $\Delta D = 32 \pm 5 \, \mu$m, angiotensin II $\Delta D = 16 \pm 1 \, \mu$m; $n = 5$; $P < 0.05$).

To independently test for the role of protein kinase C activation in the inhibition of conducted vasodilatation, either PMA or PDB was applied. Both agents produced vasoconstriction (Table 2) and inhibited conducted vaso-dilatation (Fig. 4*A*) in a manner that was also similar to the effect of phenylephrine (Fig. 3*B*); however, neither PMA nor PDB attenuated conduction to the same extent as 8 Hz SNA. Experiments with calphostin C ($n = 3$) or chelerythrine chloride ($n = 2$) to inhibit protein kinase C activity dilated vessels near-maximally, which precluded evaluation of the effect of PKC inhibition on the ability of SNA to inhibit conducted vasodilatation. Taken together, these latter findings argue for the loss of spontaneous (myogenic) vasomotor tone resulting from the inhibition of protein kinase C.

Role of membrane potential

Elevated concentrations of KCl in the superfusion solution (via equimolar replacement of NaCl) were used to effectively 'clamp' the membrane potential in a depolarized state (Hirst & van Helden, 1982) and determine how this affected conducted vasodilatation. To eliminate the possibility of stimulating α-adrenoreceptors (via depolarization of sympathetic nerve terminals), phentolamine (1 μM) was also added to the PSS. Raising $[K^+]_o$ to 30 or 40 mM produced vasoconstriction (Table 2) in the manner seen during SNA. Conducted vasodilatation was attenuated significantly in the presence of 30 mM KCl and abolished with 40 mM KCl (Fig. 4*B*). Because 40 mM KCl also diminished the local response to ACh, the ACh pulse duration was extended to 2 s, which restored local but not conducted vasodilatation. Addition of L-NNA + indomethacin further constricted vessels (to 22 $\pm$ 7 μm) and eliminated the local response to ACh yet vasodilatation to SNP was preserved ($\Delta D = 68 \pm 6 \, \mu$m; $n = 3$). Experiments using 10 or 20 mM $[K^+]_o$ resulted in either sustained vasodilatation or continuous vasomotion, which precluded further evaluation of conduction under these conditions.

Role of L-type Ca^{2+} channels

A key event in vasoconstriction produced by noradrenaline is elevation of $[Ca^{2+}]_i$ (Minneman, 1988). To test whether a rise in smooth muscle $[Ca^{2+}]_i$ underlies the inhibition of conducted vasodilatation during SNA, conduction was evaluated in the presence of Bay K 8644. Despite producing vasoconstriction similar to that of SNA (Table 2), local and conducted responses were actually enhanced by ~30% (Fig. 5*A*).

Diameter baseline controls

Our pharmacological interventions (except for UK 14,304) were associated with a reduction in baseline diameter, the magnitude of which mimicked the effect of medium (8 Hz) SNA. As an independent control for the effect of vasoconstriction on conduction, L-NNA was added to the superfusion solution. Despite eliciting vasoconstriction similar to that seen with other inter-ventions (Table 2), L-NNA had no effect on conducted vasodilatation (Fig. 5*B*). Furthermore, complementary results with prazosin present during SNA (Fig. 2*C*) or with UK 14,304 in the bath (Fig. 3*B*) indicate that the activation of α_2-adrenoreceptors inhibits conduction without changing baseline diameter (Tables 1 and 2).

NEURON simulation environment

To evaluate how changes in electrical resistive properties of the vessel wall (Fig. 6) could affect the conduction of hyper-polarization and vasodilatation along feed arteries, we modelled constant current injection into the endothelium (Emerson & Segal, 2000*a*, 2001) and electronic decay along a feed artery 'cable' (Crane *et al.* 2001). With injection of −0.25 nA, decay of hyperpolarization was minimal in the control curve (Fig. 7*A*) and accurately reflected control responses for conducted vasodilatation (Figs 1–5). Endo-thelium and smooth muscle curves were superimposed, indicating that both layers respond to current injection with similar levels of hyperpolarization (Emerson & Segal, 2001).

To model how SNA may inhibit conduction, resistive properties of the vessel (Fig. 6*C*) were varied to determine their effect on electrotonic decay. Increasing the resistance to current flow between the endothelial and smooth muscle cell layers (R_j) increased the rate of decay of hyper-polarization along the cable (Fig. 7*B*) relative to control. Under these conditions, hyperpolarization along the

endothelium was less effective in hyperpolarizing smooth muscle. Indeed, nearly 500 μm was required for respective cell layers to become isopotential. Alternatively, decreasing the resistance of the smooth muscle membrane (R_{mm}) by half (Fig. 7C) or by 10-fold (Fig. 7D) enhanced the rate of decay progressively. Furthermore, increasing R_j or decreasing R_{mm} required 4- to 16-fold greater current injection into the endothelium (with correspondingly greater hyperpolarization of the endothelium) in order to hyperpolarize adjacent smooth muscle cells to the same extent observed under control conditions (see legend to Fig. 7).

Discussion

The present study is the first to investigate the nature of interaction between conducted vasodilatation and sympathetic vasoconstriction using isolated pressurized feed arteries of the hamster retractor muscle. Each of these signalling pathways coordinates the activity of smooth muscle cells along the vessel, but does so using distinct mechanisms (Segal *et al.* 1999). Conducted vasodilatation is attributable to the initiation and conduction of hyperpolarization along the endothelium and into smooth muscle cells through myoendothelial gap junction channels (Emerson & Segal, 2000*a*,*b*). In contrast, the spread of vasoconstriction with SNA reflects initiation and propagation of action potentials along perivascular nerves, resulting in neurotransmitter release along the vessel wall (Welsh & Segal, 1996; Emerson & Segal, 2001). We show here that conducted vaso-dilatation increased with the level of ACh stimulus and decreased with the level of SNA. Thus, conduction and SNA interact dynamically and reversibly through a physiological range of vasodilatation and vasoconstriction. Furthermore, the ability of SNA to inhibit conducted vasodilatation reflects complementary effects of α_1- and α_2-adrenoreceptor-mediated signalling pathways.

Experimental design

Our strategy for these experiments was to first define the interaction between SNA and conducted vasodilatation through a full range of respective stimuli (Fig. 1). To determine whether the effects of perivascular nerve stimulation were isolated to noradrenergic innervation and to resolve the primary class of receptors involved, we then investigated the effect of non-selective inhibition of α- *versus* β-adrenoreceptors on responses to SNA and the ability of SNA to inhibit conducted vasodilatation. Since the inhibition of β-adrenoreceptors was without effect, ensuing experiments used selective α_1- or α_2-adrenoreceptor antagonists alone or in combination to evaluate the

effect of respective signalling pathways. Complementary experiments using agonists that are selective for α_1- or α_2-adrenoreceptors then determined the effect of selective activation of respective signalling pathways on conducted vasodilatation. Subsequent experiments used defined reagents to manipulate components of reported signalling pathways (Exton, 1985; Bylund, 1992; Lepretre *et al.* 1994; Guimaraes & Moura, 2001). In light of possible non-specific actions using pharmacological interventions, we reasoned that consistent outcomes across our respective interventions would strengthen conclusions regarding a particular signalling pathway.

The present findings illustrate that stimulation of α_1- and of α_2-adrenoreceptors each partially inhibits conduction, while concomitant activation of both receptor subtypes exerts a cumulative inhibitory effect with no role for β-adrenoreceptors. The ability of angiotensin II and phorbol esters to partially attenuate conduction are consistent with a role for G-protein-coupled stimulation of protein kinase C in response to SNA. In addition, the attenuation of conduction with depolarizing solutions of KCl indicates that SNA also exerts a corresponding electrical effect on cells of the vessel wall. As illustrated
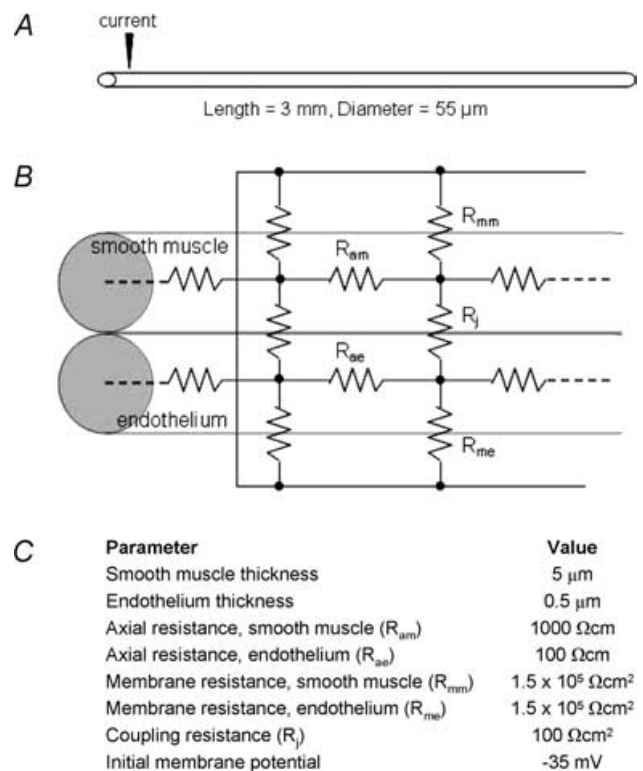

Figure 6. Modelling the biophysical properties of feed arteries as electrical 'cables'
A, schematic drawing of a feed artery showing site of current injection into endothelium (refer to Fig. 7 for outputs of model). *B*, equivalent circuit of cell layers comprising vessel wall. *C*, initial values of biophysical parameters defining control conditions.

in Figs 6 and 7, modelling feed arteries as equivalent resistive circuits indicates that multiple events initiated in smooth muscle in response to SNA can effectively impair the conduction of hyperpolarization during sympathetic neurotransmission.

Roles for α_1- and α_2-adrenoreceptors

During SNA, the partial attenuation of conduction with selective blockade of either α_1- or α_2-adrenoreceptors uniquely illustrates that distinct signalling events (Exton, 1985; Bylund, 1992; Lepretre *et al.* 1994; Guimaraes & Moura, 2001) mediate these effects (Fig. 2). Indeed, the ability of SNA to inhibit conduction was compromised when both adrenoreceptor subtypes were not stimulated simultaneously. This conclusion is strengthened by the cumulative effect of activating respective adreno-receptor subtypes with selective agonists (Fig. 3). Previous studies performed in anaesthetized hamsters (Kurjiaka & Segal, 1995; Haug *et al.* 2003) did not resolve these complementary events and the new insight gained here may be attributed to the greater control that is afforded
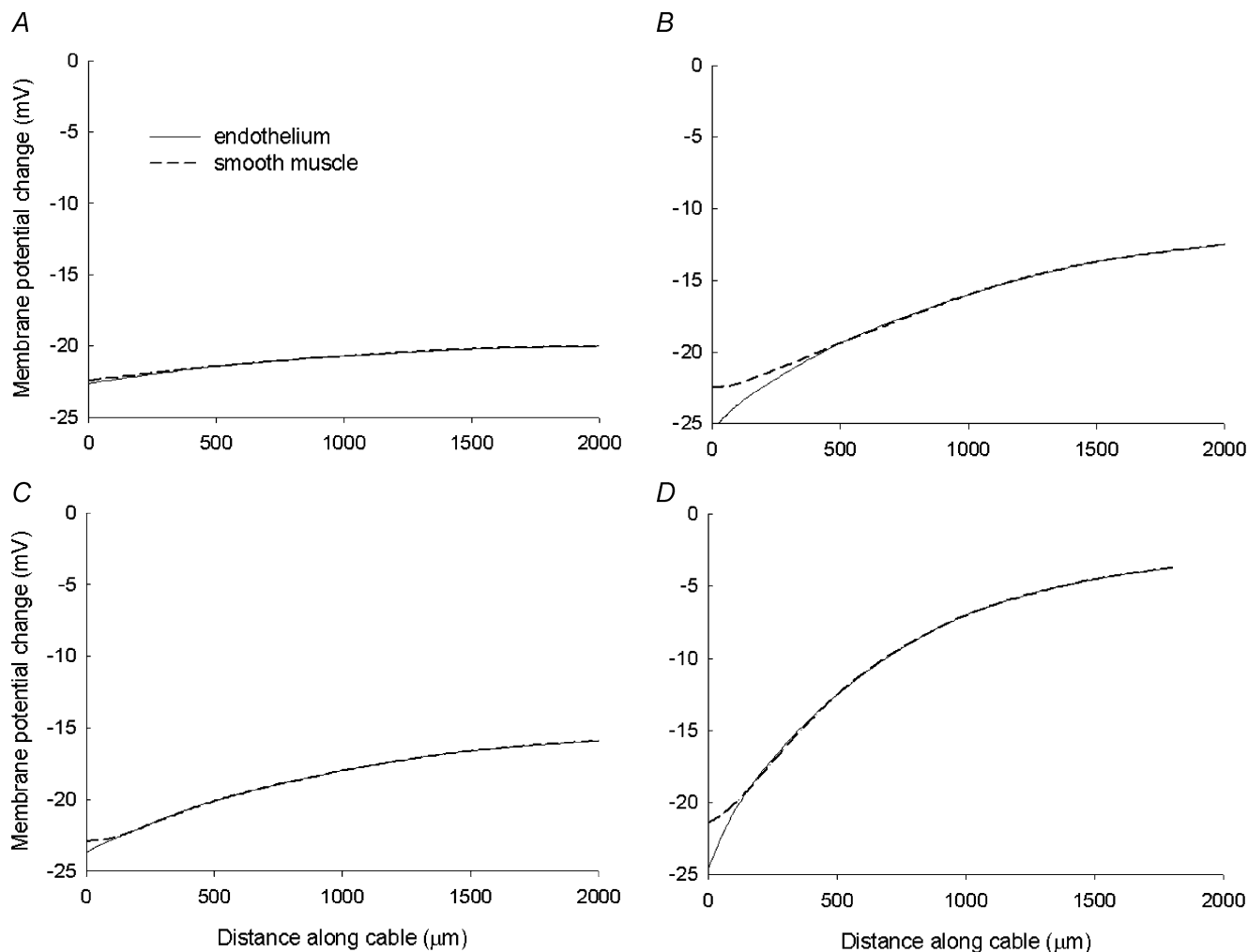

Figure 7. Simulated decay of hyperpolarization along feed artery 'cable' using NEURON
In all cases, constant current was injected into the endothelium at distance = 0 (refer to Fig. 6) and the change in membrane potential was modelled with respect to distance along the endothelium and along the smooth muscle cell layers of the 'cable'. *A*, under control conditions (defined in Fig. 6*C*), hyperpolarization is relatively constant in both cell layers along a 2000 μm segment (current injection, −0.25 nA). *B*, compared with control, increasing R_j 10-fold (to 1000 Ω cm^2) increases the difficulty of hyperpolarizing smooth muscle and increases the rate of decay of hyperpolarization (current injection, −1.5 nA). *C*, resistance of the smooth muscle cell membrane (R_{mm}) was reduced by half (to 7.5 × 10^4 Ω cm^2) compared with control (current injection, −1 nA). *D*, R_{mm} was decreased 10-fold (to 1.5 × 10^4 Ω cm^2) compared with control (current injection, −4 nA). As R_{mm} decreased (i.e. from panels *A* to *C* to *D*), hyperpolarization dissipated more rapidly along the feed artery 'cable' from the site of current injection. Note difference in amount of current injection (and endothelial cell hyperpolarization) across respective conditions to produce similar levels of smooth muscle hyperpolarization at site of stimulation.

using isolated pressurized microvessels. For example, in the presence of prazosin, conducted vasodilatation was attenuated during SNA despite the lack of vasoconstriction (Fig. 2 and Table 1), revealing an inhibitory role for α_2-adrenoreceptor activation not recognized previously. This finding is strengthened by the actions of UK 14,304, which had no effect on diameter yet attenuated conduction at remote sites (Fig. 3B). In canine and porcine coronary arteries, vasoconstriction to noradrenaline was attenuated through activation of α_2-adrenoreceptors and this effect was abolished following denudation of endothelial cells (Cocks & Angus, 1983). Thus, with the present studies performed in intact vessels, it is possible that the effects of α_2-adrenoreceptor activation in attenuating conduction were at least in part contributed by the endothelium.

In smooth muscle cells, the activation of both α_1- and α_2-adrenoreceptors can stimulate L-type Ca^{2+} channels through G_q- and G_i-protein signalling cascades, respectively (Pacaud et al. 1991; Lepretre et al. 1994). By utilizing Bay K 8644, we tested the effect of activating L-type Ca^{2+} channels on conducted vasodilatation. Remarkably, although the initial vasoconstriction was similar to that seen with SNA, vasodilatation was enhanced at both local and conducted sites (Fig. 5A). We speculate that this unexpected result may be explained by an increase in $[Ca^{2+}]_i$, acting to modulate the gating of K_{Ca} (Jaggar & Nelson, 2000; Haddock & Hill, 2002) to promote smooth muscle cell hyperpolarization and enhance dilatory responses to ACh. However, further studies are required to resolve this mechanism. In additional controls, vasoconstriction with L-NNA had no effect on conducted vasodilatation. We therefore conclude that the inhibition of conducted vasodilatation during SNA is independent of any change in the baseline diameter. This conclusion is strengthened by the ability of UK 14,304 to attenuate conduction without affecting resting diameter.

The role shown here for α_1-adrenoreceptor activation in the inhibition of conduction supports our previous findings in vivo (Kurjiaka & Segal, 1995; Haug et al. 2003). The binding of an agonist to the α_1-adrenoreceptor activates the G_q-protein signalling cascade, leading to the activation of protein kinase C (Exton, 1985; Apkon & Nerbonne, 1988). In turn, protein kinase C may modulate the conductance of gap junction channels through phosphorylation of connexin43 (Lampe et al. 2000; Bowling et al. 2001), which is highly expressed in these vessels, along with connexin37 and connexin40 (Sandow et al. 2003; Looft-Wilson et al. 2004). To further test this hypothesis, the phorbol esters PMA and PDB, which are known to activate protein kinase C (Jiang & Morgan, 1987; Nakajima et al. 1993), were each found to constrict feed arteries and inhibit conducted vasodilatation in the manner observed during stimulation

of α_1-adrenoreceptors (compare Figs 3B and 4A). These findings collectively indicate that protein kinase C can mediate the attenuation of conducted vasodilatation. However, protein kinase C can have numerous downstream effects (Lee & Severson, 1994). Thus, the precise mechanism by which kinase activation inhibits conduction remains to be established, as does the role of respective connexin protein isoforms in regulating cell-to-cell coupling along the vessel wall.

Membrane potential and vasomotor control

In response to noradrenaline, depolarization of vascular smooth muscle cells (Morgan, 1983; Nelson et al. 1988) can produce vasoconstriction by opening L-type Ca^{2+} channels (Jackson, 2000). Conversely, hyperpolarization triggered by ACh will close L-type Ca^{2+} channels and relax smooth muscle cells as it travels along the vessel wall (Jackson, 2000). Raising $[K^+]_o$ depolarizes and constricts smooth muscle cells and was therefore predicted to impair the initiation as well as the conduction of vasodilatation with ACh. We found that raising superfusate $[K^+]_o$ to 30 mM nearly abolished conducted vasodilatation at remote sites and attenuated conduction at intermediate distances along the vessel (Fig. 4). When $[K^+]_o$ was raised to 40 mM, the local response to ACh was also attenuated; increasing the ACh stimulus restored local vasodilatation but did not reverse the attenuation of conducted vasodilatation (Fig. 4). These experiments imply that depolarization of the vessel wall attenuates the conduction of hyperpolarization initiated by ACh (Emerson & Segal, 2000a,b). As verified by the addition of L-NNA + indomethacin (see Results: Role of membrane potential), the persistence of local vasodilatation during high KCl is explained by the release of endothelium-derived autacoids at the site of ACh delivery that act independently of membrane potential. In turn, the ability of vasodilatation to conduct during SNA as the ACh stimulus is raised (Fig. 1) is attributed to a correspondingly greater level of hyperpolarization (Emerson & Segal, 2000a).

The attenuation of conducted vasodilatation during SNA suggests that rate of decay of hyperpolarization along the feed artery is enhanced. One explanation for this effect is a greater resistance to current flow along the vessel wall. The endothelium serves as the principal pathway for conduction in these vessels (Emerson & Segal, 2000b). Therefore, increasing the axial resistance of the endothelium (R_{ae}) could account for the greater decay of hyperpolarization. However, the robust expression of gap junction plaques between endothelial cells (Sandow et al. 2003; Looft-Wilson et al. 2004) makes it relatively difficult to inactivate enough of these channels to reduce electrical coupling along the endothelium. In contrast, we hypothesize that noradrenaline promotes an increase in

the resistance to electrical coupling between the endothelium and smooth muscle cells (R_j), where relatively sparse gap junction plaques may be subject to physiological regulation.

With the feed artery modelled as a resistive electrical circuit (Fig. 6), the NEURON simulation environment illustrates that when R_j is increased, the ability of current derived from the endothelium to change the membrane potential of smooth muscle cells is diminished (Fig. 7*B*). Thus, the smooth muscle becomes more difficult to hyperpolarize with current originating in the endothelium (e.g. cell layers are no longer isopotential at the site of current injection) and is manifested along the vessel as a greater rate of electrical decay. Another mechanism that may explain the attenuation of conducted vasodilatation by SNA is the opening of ion channels by noradrenaline (Nelson *et al.* 1988), which will reduce the resistance of the smooth muscle cell membrane, R_{mm}. NEURON simulations of this effect illustrate that the decay of hyperpolarization increased as R_{mm} decreased (Fig. 7*C* and *D*). Taken together, these outcomes support the hypothesis that noradrenaline attenuates conducted vasodilatation by promoting the decay of hyperpolarization along the vessel wall through complementary actions: a reduction in effective myoendothelial coupling and enhanced current leak from smooth muscle cells into the extracellular fluid.

Summary

In response to contractile activity, vasodilatation ascending from arterioles into feed arteries is integral to achieving peak levels of muscle blood flow (Folkow *et al.* 1971; Segal & Jacobs, 2001). The activity of the sympathetic nervous system also increases with exercise intensity, causing vasoconstriction to resting muscle and limiting the increase in blood flow to exercising muscle (Rowell *et al.* 1996; Thomas & Segal, 2004). Thus, during intense, whole-body exercise, we suggest that by inhibiting conducted (ascending) vasodilatation in feed arteries, sympathetic nerve activation contributes to the restriction of blood flow into active skeletal muscle. The present data uniquely illustrate that conducted vasodilatation is modulated by perivascular sympathetic nerves through multiple signalling events. While these actions of SNA are mediated through the release of noradrenaline, they are independent of β-adrenoreceptors and reflect a complementary interaction between the activation of α_1- and α_2-adrenoreceptors. Modelling this interaction indicates that changes in the electrical resistance of myoendothelial gap junctions and of the smooth muscle cell membrane may serve as key sites for regulating conducted vasodilatation by sympathetic neurotransmission.

References

Aburto TK, Lajoie C & Morgan KG (1993). Mechanisms of signal transduction during alpha 2-adrenergic receptor-mediated contraction of vascular smooth muscle. *Circ Res* **72**, 778–785.

Anderson KM & Faber JE (1991). Differential sensitivity of arteriolar alpha 1- and alpha 2-adrenoceptor constriction to metabolic inhibition during rat skeletal muscle contraction. *Circ Res* **69**, 174–184.

Apkon M & Nerbonne JM (1988). Alpha 1-adrenergic agonists selectively suppress voltage-dependent K^+ current in rat ventricular myocytes. *Proc Natl Acad Sci U S A* **85**, 8756–8760.

Bowling N, Huang X, Sandusky GE, Fouts RL, Mintze K, Esterman M, Allen PD, Maddi R, McCall E & Vlahos CJ (2001). Protein kinase C-alpha and -epsilon modulate connexin-43 phosphorylation in human heart. *J Mol Cell Cardiol* **33**, 789–798.

Bylund DB (1992). Subtypes of alpha 1- and alpha 2-adrenergic receptors. *FASEB J* **6**, 832–839.

Cocks TM & Angus JA (1983). Endothelium-dependent relaxation of coronary arteries by noradrenaline and serotonin. *Nature* **305**, 627–630.

Crane GJ, Hines ML & Neild TO (2001). Simulating the spread of membrane potential changes in arteriolar networks. *Microcirculation* **8**, 33–43.

Dinh DT, Frauman AG, Johnston CI & Fabiani ME (2001). Angiotensin receptors: distribution, signalling and function. *Clin Sci* **100**, 481–492.

Emerson GG & Segal SS (2000*a*). Electrical coupling between endothelial cells and smooth muscle cells in hamster feed arteries: role in vasomotor control. *Circ Res* **87**, 474–479.

Emerson GG & Segal SS (2000*b*). Endothelial cell pathway for conduction of hyperpolarization and vasodilation along hamster feed artery. *Circ Res* **86**, 94–100.

Emerson GG & Segal SS (2001). Electrical activation of endothelium evokes vasodilation and hyperpolarization along hamster feed arteries. *Am J Physiol* **280**, H160–167.

Exton JH (1985). Mechanisms involved in alpha-adrenergic phenomena. *Am J Physiol* **248**, E633–647.

Folkow B, Sonnenschein RR & Wright DL (1971). Loci of neurogenic and metabolic effects on precapillary vessels of skeletal muscle. *Acta Physiol Scand* **81**, 459–471.

Guimaraes S & Moura D (2001). Vascular adrenoceptors: an update. *Pharmacol Rev* **53**, 319–356.

Haddock RE & Hill CE (2002). Differential activation of ion channels by inositol 1,4,5-trisphosphate (IP_3)- and ryanodine-sensitive calcium stores in rat basilar artery vasomotion. *J Physiol* **545**, 615–627.

Haug SJ, Welsh DG & Segal SS (2003). Sympathetic nerves inhibit conducted vasodilatation along feed arteries during passive stretch of hamster skeletal muscle. *J Physiol* **552**, 273–282.

Hilton SM (1959). A peripheral arterial conducting mechanism underlying dilatation of the femoral artery and concerned in functional vasodilatation in skeletal muscle. *J Physiol* **149**, 93–111.

Hines ML & Carnevale NT (1997). The NEURON simulation environment. *Neural Comput* **9**, 1179–1209.

Hirst GD & van Helden DF (1982). Ionic basis of the resting potential of submucosal arterioles in the ileum of the guinea-pig. *J Physiol* **333**, 53–67.

Jackson WF (2000). Ion channels and vascular tone. *Hypertension* **35**, 173–178.

Jaggar JH & Nelson MT (2000). Differential regulation of Ca^{2+} sparks and Ca^{2+} waves by UTP in rat cerebral artery smooth muscle cells. *Am J Physiol* **279**, C1528–1539.

Jiang MJ & Morgan KG (1987). Intracellular calcium levels in phorbol ester-induced contractions of vascular muscle. *Am J Physiol* **253**, H1365–1371.

Kurjiaka DT & Segal SS (1995). Interaction between conducted vasodilation and sympathetic nerve activation in arterioles of hamster striated muscle. *Circ Res* **76**, 885–891.

Lampe PD, TenBroek EM, Burt JM, Kurata WE, Johnson RG & Lau AF (2000). Phosphorylation of connexin43 on serine368 by protein kinase C regulates gap junctional communication. *J Cell Biol* **149**, 1503–1512.

Lee MW & Severson DL (1994). Signal transduction in vascular smooth muscle: diacylglycerol second messengers and PKC action. *Am J Physiol* **267**, C659–678.

Lepretre N, Mironneau J & Morel JL (1994). Both alpha 1A- and alpha 2A-adrenoreceptor subtypes stimulate voltage-operated L-type calcium channels in rat portal vein myocytes. Evidence for two distinct transduction pathways. *J Biol Chem* **269**, 29546–29552.

Looft-Wilson RC, Haug SJ, Neufer PD & Segal SS (2004). Independence of connexin expression and vasomotor conduction from sympathetic innervation in hamster feed arteries. *Microcirculation* **11**, 397–408.

Marshall JM (1982). The influence of the sympathetic nervous system on individual vessels of the microcirculation of skeletal muscle of the rat. *J Physiol* **332**, 169–186.

Minneman KP (1988). Alpha 1-adrenergic receptor subtypes, inositol phosphates, and sources of cell Ca^{2+}. *Pharmacol Rev* **40**, 87–119.

Morgan KG (1983). Electrophysiological differentiation of alpha-receptors on arteriolar smooth muscle. *Am J Physiol* **244**, H540–545.

Nakajima S, Fujimoto M & Ueda M (1993). Spatial changes of $[Ca^{2+}]_i$ and contraction caused by phorbol esters in vascular smooth muscle cells. *Am J Physiol* **265**, C1138–1145.

Nelson MT, Standen NB, Brayden JE, Worley JF 3rd (1988). Noradrenaline contracts arteries by activating voltage-dependent calcium channels. *Nature* **336**, 382–385.

Pacaud P, Loirand G, Baron A, Mironneau C & Mironneau J (1991). Ca^{2+} channel activation and membrane depolarization mediated by Cl^- channels in response to noradrenaline in vascular myocytes. *Br J Pharmacol* **104**, 1000–1006.

Remensnyder JP, Mitchell JH & Sarnoff SJ (1962). Functional sympatholysis during muscular activity. Observations on influence of carotid sinus on oxygen uptake. *Circ Res* **11**, 370–380.

Rowell LB, O'Leary DS & Kellog DLJ (1996). Integration of cardiovascular control systems in dynamic exercise. In *Handbook of Physiology, sect. 12, Exercise: Regulation and Integration of Multiple Systems*, pp. 770–838. Oxford University Press, New York.

Sandow SL, Looft-Wilson R, Doran B, Grayson TH, Segal SS & Hill CE (2003). Expression of homocellular and heterocellular gap junctions in hamster arterioles and feed arteries. *Cardiovasc Res* **60**, 643–653.

Segal SS & Jacobs TL (2001). Role for endothelial cell conduction in ascending vasodilatation and exercise hyperaemia in hamster skeletal muscle. *J Physiol* **536**, 937–946.

Segal SS, Welsh DG & Kurjiaka DT (1999). Spread of vasodilatation and vasoconstriction along feed arteries and arterioles of hamster skeletal muscle. *J Physiol* **516**, 283–291.

Taguchi K, Yang M, Goepel M & Michel MC (1998). Comparison of human alpha1-adrenoceptor subtype coupling to protein kinase C activation and related signalling pathways. *Naunyn Schmiedebergs Arch Pharmacol* **357**, 100–110.

Thomas GD & Segal SS (2004). Neural control of muscle blood flow during exercise. *J Appl Physiol* **97**, 731–738.

VanTeeffelen JWGE & Segal SS (2003). Interaction between sympathetic nerve activation and muscle fibre contraction in resistance vessels of hamster retractor muscle. *J Physiol* **550**, 563–574.

Welsh DG & Segal SS (1996). Muscle length directs sympathetic nerve activity and vasomotor tone in resistance vessels of hamster retractor. *Circ Res* **79**, 551–559.

Williams DA & Segal SS (1993). Feed artery role in blood flow control to rat hindlimb skeletal muscles. *J Physiol* **463**, 631–646.

Zhang H, Facemire CS, Banes AJ & Faber JE (2002). Different alpha-adrenoceptors mediate migration of vascular smooth muscle cells and adventitial fibroblasts in vitro. *Am J Physiol* **282**, H2364–2370.